Published in final edited form as:
Biol Psychiatry. 2012 May 1; 71(9): 805–813. doi:10.1016/j.biopsych.2011.06.019.

Atrophy of the cholinergic basal forebrain over the adult age range and in early stages of Alzheimer´s disease

Michel Grothe[1,*], **Helmut Heinsen**[3], and **Stefan J. Teipel**[1,2]

[1]Department of Psychiatry, University Rostock, Gehlsheimer Str. 20, 18147 Rostock, Germany

[2]DZNE, German Center for Neurodegenerative Disorders, Gehlsheimer Str. 20, 18147 Rostock, Germany

[3]Morphological Brain Research Unit, Department of Psychiatry, University Würzburg, Josef-Schneider-Str. 2, 97080 Würzburg, Germany

Abstract

Background—The basal forebrain cholinergic system (BFCS) is known to undergo moderate neurodegenerative changes during normal aging as well as severe atrophy in Alzheimer´s disease (AD). However, there is a controversy on how the cholinergic lesion in AD relates to early and incipient stages of the disease. In-vivo imaging studies on the structural integrity of the BFCS in normal and pathological aging are still rare.

Methods—We applied automated morphometry techniques in combination with high-dimensional image warping and a cytoarchitectonic map of BF cholinergic nuclei to a large cross-sectional dataset of high-resolution MRI scans, covering the whole adult age-range (20–94 years; N=211) as well as patients with very mild AD (vmAD; CDR=0.5; N=69) and clinically manifest AD (AD; CDR=1; N=28). For comparison, we investigated hippocampus volume using automated volumetry.

Results—Volume of the BFCS declined from early adulthood on and atrophy aggravated in advanced age. Volume reductions in vmAD were most pronounced in posterior parts of the nucleus basalis Meynert, while in AD atrophy was more extensive and included the whole BFCS. In clinically manifest AD, the diagnostic accuracy of BFCS volume reached the diagnostic accuracy of hippocampus volume.

Conclusions—Our findings indicate that cholinergic degeneration in AD occurs against a background of age-related atrophy and that exacerbated atrophy in AD can be detected at earliest stages of cognitive impairment. Automated in-vivo morphometry of the BFCS may become a useful tool to assess BF cholinergic degeneration in normal and pathological aging.

[*]**Corresponding Author:** Michel Grothe, Dipl.Biol., Department of Psychiatry and Psychotherapy, University Rostock, Gehlsheimer Str. 20, 18147 Rostock, Germany, Tel.: 01149-381-494-9471, Fax: 01149-381-494-9472, Michel@Grothe.org.

Parts of the presented data have been published previously as a poster at the Alzheimer´s Association International Conference on Alzheimer´s Disease (AAICAD) 2011 in Paris, France.

Financial disclosure statement
Prof. Dr. Heinsen and Mr. Grothe report no biomedical financial interests or potential conflicts of interest.

Keywords

nucleus basalis Meynert; substantia innominata; MRI; voxel-based morphometry; Mild Cognitive Impairment; OASIS

Introduction

Alzheimer´s disease (AD) is characterized by severe neurofibrillary degeneration and cell loss of the basal forebrain cholinergic system (BFCS), which is accompanied by loss of cortical cholinergic innervation (1, 2, 3, 4). Several lines of evidence suggest that the cholinergic lesion in AD is, at least partly, responsible for the specific cognitive impairments in memory, attention and executive function (5, 6, 7).

However, it is still under debate how cholinergic impairment relates to early or incipient stages of the disease (8). In mild stages of AD, post-mortem studies suggest no loss of cortical choline acetyl transferase (ChAT) activity or reduced numbers of cholinergic neurons in the nucleus basalis Meynert (NBM) (9, 10). In mild cognitive impairment (MCI), a clinical at risk stage of AD (11), ChAT activity in the hippocampus and the frontal cortex was even increased when compared to controls (12). On the other hand, NBM cholinergic neurons are highly sensitive to age-related neurofibrillary degeneration and show early cytoskeletal changes in the form of neurofibrillary tangles (13, 14, 15). Furthermore, number and size of BF cholinergic neurons as well as activity of cortical cholinergic markers were found to decrease along the human lifespan, suggesting that the cholinergic degeneration in AD may occur against a background of considerable age-related atrophy (2, 3, 16, 17).

Neuroimaging-derived measures of BF structural integrity provide the potential to indirectly assess BF cholinergic degeneration in the human brain in-vivo. A first approach to in-vivo morphometry of the BF employed manual measurement of the thickness of the substantia innominata (SI) on a coronal section at the level of the anterior commissure (18). Two recent studies using similar manual volumetry protocols reported contradictory results in respect to reduced volumes of the SI in mild AD and MCI (19, 20). However, these manual volumetry protocols are restricted to a small well-delineable part of the BFCS centered on the anterior commissure. Thus, they provide a very rough estimate of atrophy of the BFCS, which extends about 20 mm in anterior-posterior direction (21, 22, 23).

The recent development of stereotaxic cytoarchitectonic maps of BF cholinergic nuclei based on combined MRI and histology of post-mortem brains (22, 23) opened the door for automated in-vivo morphometry of the BFCS. Using high-dimensional deformation based morphometry techniques in combination with these cytoarchitectonic maps, we could detect reduced volumes of the cholinergic BF in AD as well as in two independent samples of MCI patients (24, 25). Reduced volumes on a voxel-basis were less pronounced in MCI compared to AD but mapped to similar locations of the cholinergic space, most notably posterior parts of the NBM. Here we applied a highly automated voxel-based morphometry approach in combination with high-dimensional image warping to a publicly available cross-sectional dataset of 308 high-contrast MR images covering the whole adult lifespan as well as early stages of AD (26). Effects of age-related grey matter (GM) degeneration on a voxel-basis were mapped to the BFCS using a cytoarchitectonic map of BF cholinergic nuclei (22). Furthermore, individual volumes of the BFCS were automatically extracted to estimate the effect of age on volume. By contrasting samples of clinically manifest AD (CDR = 1) and very mild/questionable AD (CDR = 0.5) with an age-matched sub-sample of the healthy cohort we assessed the additional effect of AD pathology on BFCS atrophy at different stages of disease severity. The diagnostic use of BFCS atrophy to discriminate different

stages of AD from healthy aging was compared to the diagnostic accuracy of hippocampus atrophy, to date the best established structural marker of AD (27).

Material and Methods

Subjects

Magnetic resonance imaging (MRI) scans were retrieved from the open-source OASIS-database (26; http://www.oasis.org) and included 211 healthy individuals (20–94 years) as well as 28 subjects with clinically manifest AD (CDR = 1, MMSE = 21.7±3.8, 77.8±7.0; AD) and 69 subjects with very mild/questionable AD (CDR = 0.5, MMSE = 25.6±3.5, age = 76.2±7.2; vmAD). Demographics and global neuropsychological profiles of the studied samples are summarized in Table S1 in the Supplement. MMSE scores of both patient groups differed significantly ($p < 0.001$) from the control group of healthy elderly, including all healthy individuals aged 60 or older (MMSE = 29.0±1.2, age = 75.6±8.9), as well as from each other ($p < 0.001$). Neither the vmAD group nor the AD group differed significantly in age from the control group ($p = 0.3$ and $p = 0.09$, for vmAD and AD, respectively). Detailed inclusion- and diagnostic criteria of the OASIS-database are described in the OASIS documentation (26) and specific selection criteria for the studied sample here are described in the Supplement. Briefly, all subjects participated in accordance with guidelines of the Washington University Human Studies Committee. Approval for public sharing of the data was also specifically obtained. Participants were clinically screened and exclusion criteria included use of psychoactive drugs, serious head injury, history of clinically meaningful stroke, active neurological or psychiatric illness as well as primary causes of dementia other than AD. Older adults, aged 60 or older, underwent full clinical assessment and dementia status was established and staged using the Clinical Dementia Rating (CDR) scale (28, 29). Following the staging of AD based on CDR scores, a global CDR of 0 indicates no dementia, and CDRs of 0.5, 1, 2, and 3 represent very mild, mild, moderate, and severe dementia, respectively (30, 31). Based on a CDR score of 0.5 (questionable dementia), vmAD represents a mild level of cognitive impairment that does not suffice for the diagnosis of clinically manifest AD (32). Although this classification differs slightly from the Petersen-criteria for the diagnosis of MCI (11), autopsy studies suggest that the diagnoses of vmAD and MCI represent similar levels of early AD pathology (33, 34, 35).

MRI acquisition

All images of the OASIS-database were acquired on a 1.5-T Vision scanner (Siemens, Erlangen, Germany) using a T1-weighted magnetization prepared rapid gradient-echo (MP-RAGE) sequence with empirically optimized parameters for grey-white contrast. For each subject, 3–4 individual T1-weighted MP-RAGE images were acquired in a single imaging session and averaged subsequently, resulting in high signal to noise ratios for the individual scans. More detailed information on the acquisition procedure and scanning parameters can be found in (26) and the Supplement.

MRI processing

Main processing steps and computational analyses employed in the present study are summarized in Figure S1 in the Supplement. MRI data were processed by using statistical parametric mapping (SPM8, Wellcome Trust Center for Neuroimaging) and the VBM8-toolbox (http://dbm.neuro.uni-jena.de/vbm/) implemented in MatLab R2007a (MathWorks, Natick, MA).

First, images were segmented into GM, white matter (WM) and cerebrospinal fluid (CSF) partitions using the tissue prior free segmentation routine of the VBM8-toolbox. The

resulting GM and WM partitions of each subject in native space were then high-dimensionally registered to study population-specific templates using DARTEL (36). For the study of age-effects on GM volume over the adult lifespan, tissue-partitions of all 211 healthy subjects were registered to their anatomic mean, resulting in a "lifespan-template". Structural brain characteristics change considerably in advanced age and AD and spatial registration accuracy worsens with deviance from the template characteristics. Thus, for the study of GM degeneration in AD compared to healthy elderly, tissue-partitions of equal portions of the three diagnostic groups (healthy elderly, mAD and vmAD, 28 subjects each) were registered together, resulting in the "elderly-AD-template". Remaining subjects were registered to this representative template of the group mean anatomy.

For both templates, representing the respective average anatomies in native space, an affine transform to MNI standard space was calculated. These affine transforms were combined with the individual flow-fields resulting from the DARTEL registrations and the combined transforms were used to warp the GM segments to the respective reference anatomy in MNI space. Voxel-values were modulated for volumetric changes introduced by the high-dimensional normalization, such that the total amount of GM volume present before warping was preserved. Finally, modulated warped GM segments were resliced to an isotropic voxel-size of $1mm^3$ and smoothed with a Gaussian smoothing kernel of 4mm full-width at half maximum (FWHM).

Individual GM volumes of the BFCS as well as the hippocampus were extracted automatically by summing up the modulated GM voxel values within the respective ROI mask in the reference space (see below). For further analyses, the extracted BFCS and hippocampus GM volumes were normalized by the total intracranial volume (TIV), calculated as the sum of total volumes of the GM, WM and CSF partitions.

Definition of the BFCS and hippocampus regions-of-interest

The ROI masks for the hippocampus were obtained by separate manual delineation of the hippocampus in the two different reference spaces using the interactive software package Display (McConnell Brain Imaging Centre at the Montreal Neurological Institute) and a previously described protocol for segmentation of the medial temporal lobe (MTL) (37). The BFCS is composed of four groups of cholinergic cells. According to Mesulam´s nomenclature, Ch1 refers to the cholinergic cells associated with the medial septal nucleus, Ch2 and Ch3 to those belonging to the vertical and horizontal limb of the diagonal band of Broca (DB), respectively, and Ch4 designates the cholinergic cells within the NBM (38). The NBM is the largest nucleus of the BFCS and can be further subdivided into anterior lateral (Ch4al) and medial (Ch4am), intermediate (Ch4i) and posterior regions (Ch4p). The cholinergic nuclei lack clear anatomical borders that could be easily identified on MRI scans, rendering manual delineation impractical. The BFCS-masks used in this study were therefore based on a cytoarchitectonic map of BF cholinergic nuclei in MNI space, derived from combined histology and MRI of a post-mortem brain (22). Please refer to the Supplement for more detailed information on the cytoarchitectonic map and the generation of study-specific masks for the hippocampus and BFCS.

Statistical analysis

For voxel-wise statistical analyses we employed the general linear model on a voxel-basis within the SPM framework. Regression analyses and group-wise comparisons (t-tests) of TIV-normalized BFCS and hippocampus GM volumes were performed using Statistics Software Package for the Social Sciences (SPSS v15.0). Diagnostic performance of the volumetric measures were assessed and statistically compared using area under the curve

(AUC)-values of receiver operating characteristics (ROC) analyses implemented in ROCKIT-software (Kurt Rossmann Laboratories; 39, 40).

The effects of age on BFCS GM degeneration were determined using multiple linear regression of age on the preprocessed GM maps of the healthy individuals with gender and TIV as confounding variables. The voxel-wise analysis was restricted to the BFCS-ROI. Results were assessed at a statistical threshold of $p < 0.01$, corrected for multiple comparisons using the false discovery rate (FDR), and a minimum cluster extension threshold of 5 contiguous voxels was applied. A separate analysis was run using the same model but controlling for total GM volume instead of TIV.

In addition we determined linear and quadratic regression models for the effect of age on TIV-normalized segmented BFCS and hippocampus GM volumes for the whole group of healthy subjects (20–94 years).

To examine the progressive character of region-specific neurodegeneration in the course of AD we compared the AD and vmAD groups, respectively, with an age-matched subsample of the healthy cohort. The contrast used a voxel-wise ANCOVA model with diagnosis as variable of interest and age, gender and TIV as confounding variables. Analysis was restricted to the BFCS-ROI and results were assessed at an FDR-corrected statistical threshold of $p < 0.01$, with a minimum cluster extension threshold of 5 contiguous voxels. A separate analysis was run using the same model but controlling for total GM volume instead of TIV.

The power of individual BFCS and hippocampus GM volumes to discriminate between healthy elderly and different stages of AD was assessed by calculating ROC-curves between both groups of AD-severity (vmAD and AD) and the healthy elderly control group. Potentially additive discriminative effects of the single structural markers were examined using a composite marker, calculated as the arithmetic mean of TIV-normalized BFCS and hippocampus GM volumes divided by their respective mask size.

Results

Age-related GM loss within the BFCS

Results of the voxel-wise linear regression analysis between age and GM volume of the BFCS are shown in Figure 1. Significant age-related reductions of bilateral GM volume within the BFCS were detected throughout the whole ROI, including the vertical (Ch2) and horizontal (Ch3) limb of the DB as well as anterior, intermediate and posterior parts of the NBM (Ch4). Peak effects of age-related volume decline are listed in Table S2 in the Supplement. They corresponded to anterior lateral (Ch4al), medial (Ch4am) and intermediate (Ch4i) parts of the NBM as well as to the vertical limb of the DB (Ch2). Results remained virtually unchanged when controlling for total GM instead of TIV (data not shown).

Total TIV-normalized GM volumes of the BFCS for young to middle aged adults (20–59 years) were 405 mm^3 and 383 mm^3, for left and right BFCS, respectively. Average GM volumes of left and right BFCS for subjects aged 60 or older were 368 mm^3 and 339 mm^3, respectively. BFCS volumes differed significantly between hemispheres in both age groups ($p < 0.001$, for both young to middle aged and older subjects) as well as between age-groups ($p < 0.001$, for both left and right hemisphere). In Figure 2 normalized GM volumes of left and right BFCS and hippocampus are plotted against age. Qualitatively, the plot revealed a moderate decline of BFCS GM volume from early adulthood to middle-age and increasing decline at advanced age with an inflection point at a critical age of approximately 65–70

years. The linear regression model yielded average rates of decline of 0.23%/year for the left (R^2 = 0.277, F = 80.2, p < 0.001) and 0.28%/year for the right BFCS (R^2 = 0.350, F = 112.3, p < 0.001), the age-by-hemisphere interaction being non-significant (p = 0.26). Inclusion of a quadratic term significantly improved the fit of the model (R^2 = 0.320, dF = 13.0, p < 0.001 and R^2 = 0.395, dF = 15.6, p < 0.001, for left and right BFCS, respectively). The plots of hippocampus GM volumes against age revealed stable (or even increasing) volumes from early adulthood to middle age followed by a decline of volume at advanced age. Hence, the fit of a linear regression model was significantly inferior (R^2 = 0.016, F = 3.4, p = 0.07 and R^2 = 0.011, F = 2.4, p = 0.12, for left and right hippocampus, respectively) to the fit of a model including a quadratic term (R^2 = 0.190, dF = 44.7, p < 0.001 and R^2 = 0.173, dF = 40.6, p < 0.001).

Atrophy of the BFCS at early stages of AD

In the vmAD group, voxel-wise effects of reduced GM volumes, corresponded to bilateral posterior (Ch4p), anterior lateral (CH4al) and intermediate parts (Ch4i) of the NBM (Figure 3 and Table S3 in the Supplement). In the right hemisphere, there were additional effects corresponding to the anterior medial NBM (Ch4am) and the horizontal limb of the DB (Ch3). Voxel-wise effects of reduced GM volumes in the AD group were more extensive than in the vmAD group and were detected throughout the whole BFCS-ROI, including the vertical (Ch2) and horizontal limb (Ch3) of the DB as well as the whole extent of the NBM (Ch4) (Figure 4 and Table S4 in the Supplement). In both groups, peak-effects of reduced volumes of the BFCS were most pronounced in posterior parts of the NBM (Ch4p). When controlling for total GM volume instead of TIV, effects in the AD group remained significant for the whole BFCS-ROI with the exception of most anterior medial regions, mainly corresponding to the vertical limb of the DB (Ch2). In the vmAD group, effects of reduced volume only remained significant in posterior parts of the NBM (Tables S5 and S6 in the Supplement).

Diagnostic power of BFCS- and hippocampus atrophy at different stages of dementia severity

Total TIV-normalized GM volumes of the BFCS and the hippocampus were significantly different between both AD groups (AD and vmAD) and the age- and gender-matched control group (Table 1). Compared to healthy elderly, bilateral BFCS and hippocampus GM volumes of the vmAD group showed an average volume reduction of 6.8% (p < 0.001) and 10.3% (p < 0.001), respectively. In the AD group, average BFCS and hippocampus GM volumes were reduced by 14.5% (p < 0.001) and 14.2% (p < 0.001), respectively, relative to the healthy control group.

For the distinction between vmAD and healthy elderly controls, diagnostic power of bilateral BFCS GM volume with an AUC of 0.69 was significantly inferior to the diagnostic power of hippocampus GM volume with an AUC of 0.78 (p = 0.01 for difference between the AUCs). However, in the AD group the diagnostic accuracy of BFCS GM volume reached the same diagnostic accuracy as hippocampus GM volume with an AUC of 0.81 for both measures (p > 0.5 for the difference in AUCs between markers). While diagnostic performance of hippocampus GM volume did not differ significantly between the two patient groups (p = 0.3), the increase in diagnostic accuracy of BFCS GM volume for the detection of AD compared to the detection of vmAD was statistically significant (p = 0.02). The composite marker of combined BFCS and hippocampus volumes significantly increased the diagnostic accuracy for discrimination between AD and healthy controls (AUC = 0.87; p = 0.04 and p = 0.01, compared to diagnostic power of hippocampus and BFCS GM volume, respectively) but not for the separation of vmAD and healthy controls (AUC = 0.76).

Discussion

Here we demonstrate age-related decline of BFCS GM volume that begins in early adulthood and aggravates in advanced age. The effects of age on BFCS GM volume were preserved, even when effects of age on overall cerebral GM volume were taken into account. Although there is only little evidence from structural in-vivo neuroimaging studies so far (18), age-related decreases of BF cholinergic neuron number and size starting early in adult life have been reported by a range of post-mortem studies in animal-models (5, 6) and human brain specimens (2, 16, 17). Interestingly, the reported 20–30% reduction of cholinergic cells in the 9th decade compared to newborns fits well with our findings of estimated annual atrophy rates between 0.23% and 0.28%. However, there is now ample evidence that age-related cholinergic dysfunction is mediated mainly by decreased cellular function and brain choline uptake and associated neuronal shrinkage, axonal degeneration and synaptic loss, rather than definite cell loss [41, 42]. It has been hypothesized that when the increasing functional and structural alterations of the BFCS exceed a certain threshold, they mediate, or contribute to, the cognitive deficits in memory and attention/executive function associated with advanced age (17, 43, 44, 45).

We further replicate and extend our previous findings of reduced volumes of the BFCS at earliest stages of AD compared to age-matched controls, predominantly affecting posterior to intermediate parts of the NBM (24, 25). At the cognitively more impaired stage of clinically manifest AD, effects of reduced volume were found to be much more extended into rostral regions and included virtually all parts of the BFCS. Although there is increasing agreement on the course of cortical atrophy in AD (46, 47), the involvement of the BFCS across age and disease stages has been little explored and current in-vivo findings on the structural integrity of the BFCS at early stages of AD are contradictory (19, 20, 24, 25). The existing post-mortem data indicate that although definite cell loss may be less prominent, considerable functional and structural disturbances of the BFCS, including impaired trophic support and protein synthesis, tauopathy and cytoskeletal abnormalities, occur early in the course of AD (13, 14, 15, 48, 49). This is also supported by recent imaging studies that found cortical cholinergic markers other than ChAT-activity, including acetylcholine esterase activity and vesicular acetylcholine transporter binding, to be substantially reduced at early stages of AD (50, 51, 52). Based on post-mortem findings of most severe atrophy over posterior parts of the NBM, it has been hypothesized that the specific vulnerability of the BFCS to AD pathology may be due to its anatomical position and structural connections with early and severely affected structures of the MTL, including entorhinal cortex, amygdala and hippocampus (8). Our findings of the voxel-wise analyses lend further support to the hypothesis of spreading atrophy from the MTL over posterior to anterior parts of the BFCS. Moreover, this progression of atrophy seems to occur early in the disease progress, at the transition from very mild to clinically manifest AD.

The diagnostic power of BFCS volume was significantly inferior to the diagnostic power of hippocampus volume in the vmAD group compared to healthy controls. However, the increased atrophy of the BFCS in the AD group rendered BFCS GM volume a useful diagnostic marker for the first CDR-stage of clinically manifest AD, yielding equal diagnostic accuracies as hippocampus GM volume. Moreover, the increased diagnostic accuracy of a composite marker of combined BFCS and hippocampus GM volume in the AD group suggests that BFCS volumetry may be of additional value for imaging marker-based diagnosis of AD. There are no reference data for in-vivo measures of BFCS volume, but hippocampus volume reductions and their diagnostic potentials found in the present study match well with previous results from automated as well as manual volumetry studies on early AD and MCI (55, 56, 57).

The cross-sectional design of the present study to estimate the course of age-related neurodegeneration along the whole adult lifespan is prone to potential secular changes in brain size and structural integrity. Furthermore, there are no longitudinal follow-up data available, and thus the degree of undetected AD pathology in the healthy elderly cohort is unknown. Also, differences in atrophy rates of the BFCS and hippocampus between healthy elderly and early stages of AD may be more appropriate measures than baseline volumes to discriminate between diagnostic groups (58). Longitudinal imaging designs are needed to substantiate the dynamics of BFCS atrophy in elderly subjects.

By drawing inference from in-vivo MR images instead of post mortem brain specimens, the present study faces some technical limitations. Firstly, on the basis of the measured MR signal it cannot be decided whether the detected volume reductions reflect neuronal shrinkage or definite cell loss. Furthermore, the BF cholinergic space is not directly visible in MR scans, and therefore the definition of the BFCS-ROI in this study has to rely on an indirect localization of the cholinergic space by a cytoarchitectonic map derived from a single-subject normalized to MNI space (22). Probabilistic cytoarchitectonic maps of cholinergic nuclei that incorporate information about inter-individual variance have been developed recently (23) and successfully applied to the study of BFCS volume reductions in MCI (25). Unfortunately, these probabilistic maps of the BFCS are not publicly available yet, which is why we decided to use our single-subject map in the present study. However, the reported data for the probabilistic maps (e.g. center-of-gravity coordinates of the different cholinergic nuclei) show very good overlap with our single-subject map and differences between the two maps were judged to be of minor importance compared to the resolution of MRI-based in-vivo morphometry.

In summary, by using up-to-date automated morphometry techniques in combination with a cytoarchitectonic map of the BFCS we demonstrated a moderate structural decline of the BFCS along the adult lifespan that worsens in advanced age. Early stages of AD led to a further decrement of BFCS volume beyond the age effect alone. Our cross-sectional data suggest that exacerbated volume reductions of the BFCS in AD start in posterior parts of the NBM at earliest stages of cognitive impairment and spread to include more rostral regions in patients with clinically manifest AD. The marked reduction of BFCS volume in clinically manifest AD demonstrated to be of additional diagnostic value over and above volumetry of the hippocampus. The BFCS is an important target site for AD drug development and a promising treatment approach to date aims at restoring the disrupted trophic support in the BFCS by nerve growth factor gene delivery (59, 60). Beyond its use as structural marker for imaging-based diagnosis of AD, automated in-vivo measurement of BFCS structural integrity may also be an import tool to monitor the effects of drugs that target the BFCS.

Supplementary Material

Refer to Web version on PubMed Central for supplementary material.

Acknowledgments

Funding/Acknowledgments

Part of this work was supported by grants from the Interdisciplinary Faculty, Department “Ageing Science and Humanities”, University of Rostock, to S.J.T. and of the Hirnliga e. V. (Nürmbrecht, Germany) to S.J.T. The present study has been made possible through the free availability of MRI data sets from the Open Access Series of Imaging Studies (OASIS). OASIS is made available by the Washington University Alzheimer’s Disease Research Center, Dr. Randy Buckner at the Howard Hughes Medical Institute (HHMI) at Harvard University, the Neuroinformatics Research Group (NRG) at Washington University School of Medicine, and the Biomedical Informatics Research Network (BIRN) [Grant numbers P50 AG05681, P01 AG03991, R01 AG021910, P50 MH071616, U24 RR021382, R01 MH56584].

Prof. Dr. Teipel reports having received grants from the Interdisciplinary Faculty, Department “Ageing Science and Humanities”, University of Rostock, and the Hirnliga e. V. (Nürmbrecht, Germany).

References

1. Lehericy S, Hirsch EC, Cervera-Pierot P, Hersh LB, Bakchine S, Piette F. Heterogeneity and selectivity of the degeneration of cholinergic neurons in the basal forebrain of patients with Alzheimer’s disease. J Comp Neurol. 1993; 330:15–31. [PubMed: 8468401]
2. McGeer PL, McGeer EG, Suzuki J, Dolman CE, Nagai T. Aging, Alzheimer’s disease, and the cholinergic system of the basal forebrain. Neurology. 1984; 34:741–745. [PubMed: 6539435]
3. Perry EK. The cholinergic system in old age and Alzheimer's disease. Age Ageing. 1980; 9(1):1–8. [PubMed: 7361631]
4. Whitehouse PJ, Price DL, Clark AW, Coyle JT, DeLong MR. Alzheimer disease: Evidence for selective loss of cholinergic neurons in the nucleus basalis. Ann Neurol. 1981; 10:122–126. [PubMed: 7283399]
5. Bartus RT. On neurodegenerative diseases, models, and treatment strategies: lessons learned and lessons forgotten a generation following the cholinergic hypothesis. Exp Neurol. 2000; 163(2):495–529. Review. [PubMed: 10833325]
6. Muir JL. Acetylcholine, aging, and Alzheimer's disease. Pharmacol Biochem Behav. 1997; 56(4): 687–696. Review. [PubMed: 9130295]
7. Sarter M, Bruno JP, Givens B. Attentional functions of cortical cholinergic inputs: what does it mean for learning and memory? Neurobiol Learn Mem. 2003; 80(3):245–256. Review. [PubMed: 14521867]
8. Mesulam M. The cholinergic lesion of Alzheimer’s disease: pivotal factor or side show? Learn Mem. 2004a; 11:43–49. [PubMed: 14747516]
9. Gilmor ML, Erickson JD, Varoqui H, Hersh LB, Bennett DA, Cochran EJ, et al. Preservation of nucleus basalis neurons containing choline acetyltransferase and the vesicular acetylcholine transporter in the elderly with mild cognitive impairment and early Alzheimer’s disease. J Comp Neurol. 1999; 411:693–704. [PubMed: 10421878]
10. Tiraboschi P, Hansen LA, Alford M, Masliah E, Thal LJ, Corey-Bloom J. The decline in synapses and cholinergic activity is asynchronous in Alzheimer's disease. Neurology. 2000; 55(9):1278–1283. [PubMed: 11087768]
11. Gauthier S, Reisberg B, Zaudig M, Petersen RC, Ritchie K, Broich K, et al. Cognitive Impairment International Psychogeriatric Association Expert Conference on mild cognitive impairment (2006): Mild Cognitive Impairment. Lancet. 367(9518):1262–1270. Review. [PubMed: 16631882]
12. DeKosky ST, Ikonomovic MD, Styren SD, Beckett L, Wisniewski S, Bennett DA, et al. Upregulation of choline acetyltransferase activity in hippocampus and frontal cortex of elderly subjects with mild cognitive impairment. Ann Neurol. 2002; 51:145–155. [PubMed: 11835370]
13. Geula C, Nagykery N, Nicholas A, Wu CK. Cholinergic neuronal and axonal abnormalities are present early in aging and in Alzheimer disease. J Neuropathol Exp Neurol. 2008; 67(4):309–318. [PubMed: 18379437]
14. Mesulam M, Shaw P, Mash D, Weintraub S. Cholinergic nucleus basalis tauopathy emerges early in the aging-MCI-AD continuum. Ann Neurol. 2004; 55(6):815–828. [PubMed: 15174015]
15. Sassin I, Schultz C, Thal DR, Rüb U, Arai K, Braak E, et al. Evolution of Alzheimer’s disease-related cytoskeletal changes in the basal nucleus of Meynert. Acta Neuropathologica. 2000; 100:259–269. [PubMed: 10965795]
16. Lowes-Hummel P, Gertz HJ, Ferszt R, Cervos-Navarro J. The basal nucleus of Meynert revised: the nerve cell number decreases with age. Arch Gerontol Geriatr. 1989; 8:21–27. [PubMed: 2712647]
17. Mann DM, Yates PO, Marcyniuk B. Changes in nerve cells of the nucleus basalis of Meynert in Alzheimer's disease and their relationship to ageing and to the accumulation of lipofuscin pigment. Mech Ageing Dev. 1984; 25(1–2):189–204. [PubMed: 6202988]

18. Hanyu H, Asano T, Sakurai H, Tanaka Y, Takasaki M, Abe K. MR analysis of the substantia innominata in normal aging, Alzheimer disease, and other types of dementia. AJNR Am J Neuroradiol. 2002; 23:27–32. [PubMed: 11827872]
19. George S, Mufson EJ, Leurgans S, Shah RC, Ferrari C, Detoledo-Morrell L. MRI-based volumetric measurement of the substantia innominata in amnestic MCI and mild AD. Neurobiol Aging. (in press) [Epub ahead of print].
20. Muth K, Schönmeyer R, Matura S, Haenschel C, Schröder J, Pantel J. Mild cognitive impairment in the elderly is associated with volume loss of the cholinergic basal forebrain region. Biol Psychiatry. 2010; 67(6):588–591. [PubMed: 19375072]
21. Halliday GM, Cullen K, Cairns MJ. Quantitation and three-dimensional reconstruction of Ch4 nucleus in the human basal forebrain. Synapse. 1993; 15:1–16. [PubMed: 8310421]
22. Teipel SJ, Flatz WH, Heinsen H, Bokde AL, Schoenberg SO, Stockel S, et al. Measurement of basal forebrain atrophy in Alzheimer's disease using MRI. Brain. 2005; 128(Pt 11):2626–2644. [PubMed: 16014654]
23. Zaborszky L, Hoemke L, Mohlberg H, Schleicher A, Amunts K, Zilles K. Stereotaxic probabilistic maps of the magnocellular cell groups in human basal forebrain. Neuroimage. 2008; 42(3):1127–1141. [PubMed: 18585468]
24. Teipel SJ, Meindl T, Grinberg L, Grothe M, Cantero JL, Reiser MF, et al. The cholinergic system in mild cognitive impairment and Alzheimer's disease: An in vivo MRI and DTI study. Hum Brain Mapp. (in press) [Epub ahead of print].
25. Grothe M, Zaborszky L, Atienza M, Gil-Neciga E, Rodriguez-Romero R, Teipel SJ, et al. Reduction of basal forebrain cholinergic system parallels cognitive impairment in patients at high risk of developing Alzheimer's disease. Cereb Cortex. 2010; 20(7):1685–1695. [PubMed: 19889714]
26. Marcus DS, Wang TH, Parker J, Csernansky JG, Morris JC, Buckner RL. Open Access Series of Imaging Studies (OASIS): cross-sectional MRI data in young, middle aged, nondemented, and demented older adults. J Cogn Neurosci. 2007; 19(9):1498–1507. [PubMed: 17714011]
27. Teipel SJ, Meindl T, Grinberg L, Heinsen H, Hampel H. Novel MRI techniques in the assessment of dementia. Eur J Nucl Med Mol Imaging. 2008; 35(Suppl 1):S58–S69. Review. [PubMed: 18205002]
28. McKhann G, Drachman D, Folstein M, Katzman R, Price D, Stadlan EM. Clinical diagnosis of Alzheimer's disease: report of the NINCDS-ADRDA Work Group under the auspices of Department of Health and Human Services Task Force on Alzheimer's Disease. Neurology. 1984; 34(7):939–944. [PubMed: 6610841]
29. Morris JC. The Clinical Dementia Rating (CDR): current version and scoring rules. Neurology. 1993; 43(11):2412–2414. [PubMed: 8232972]
30. Berg L, Hughes CP, Coben LA, Danziger WL, Martin RL, Knesevich J. Mild senile dementia of Alzheimer type: research diagnostic criteria, recruitment, and description of a study population. J Neurol Neurosurg Psychiatry. 1982; 45(11):962–968. [PubMed: 7175540]
31. Berg L, McKeel DW Jr, Miller JP, Storandt M, Rubin EH, Morris JC, et al. Clinicopathologic studies in cognitively healthy aging and Alzheimer's disease: relation of histologic markers to dementia severity, age, sex, and apolipoprotein E genotype. Arch Neurol. 1998; 55(3):326–335. [PubMed: 9520006]
32. Morris JC, McKeel DW Jr, Storandt M, Rubin EH, Price JL, Grant EA, et al. Very mild Alzheimer's disease: informant-based clinical, psychometric, and pathologic distinction from normal aging. Neurology. 1991; 41(4):469–478. [PubMed: 2011242]
33. Morris JC, Storandt M, Miller JP, McKeel DW, Price JL, Rubin EH, et al. Mild cognitive impairment represents early-stage Alzheimer disease. Arch Neurol. 2001; 58(3):397–405. [PubMed: 11255443]
34. Morris JC, Price AL. Pathologic correlates of nondemented aging, mild cognitive impairment, and early-stage Alzheimer's disease. J Mol Neurosci. 2001; 17(2):101–118. Review. [PubMed: 11816784]
35. Storandt M, Grant EA, Miller JP, Morris JC. Longitudinal course and neuropathologic outcomes in original vs revised MCI and in pre-MCI. Neurology. 2006; 67(3):467–473. [PubMed: 16894109]

36. Ashburner J. A fast diffeomorphic image registration algorithm. Neuroimage. 2007; 38(1):95–113. [PubMed: 17761438]
37. Pruessner JC, Li LM, Serles W, Pruessner M, Collins DL, Kabani N, et al. Volumetry of hippocampus and amygdala with high-resolution MRI and three-dimensional analysis software: minimizing the discrepancies between laboratories. Cereb Cortex. 2000; 10(4):433–442. [PubMed: 10769253]
38. Mesulam MM, Mufson EJ, Wainer BH, Levey AI. Central cholinergic pathways in the rat: An overview based on an alternative nomenclature (Ch1–Ch6). Neuroscience. 1983; 10:1185–1201. [PubMed: 6320048]
39. Metz, CE. Statistical analysis of ROC data in evaluating diagnostic performance. In: Herbert, D.; Myers, R., editors. Multiple regression analysis: applications in the health sciences. New York: American Institute of Physics; 1986. p. 365
40. Metz CE, Herman BA, Roe CA. Statistical comparison of two ROC curve estimates obtained from partially-paired datasets. Med Decis Making. 1998; 18:110. [PubMed: 9456215]
41. Cohen BM, Renshaw PF, Stoll AL, Wurtman RJ, Yurgelun-Todd D, Babb SM. Decreased brain choline uptake in older adults. An in vivo proton magnetic resonance spectroscopy study. JAMA. 1995; 274(11):902–907. [PubMed: 7674505]
42. Schliebs R, Arendt T. The cholinergic system in aging and neuronal degeneration. Behav Brain Res. (in press) [Epub ahead of print].
43. Schliebs R, Arendt T. The significance of the cholinergic system in the brain during aging and in Alzheimer's disease. J Neural Transm. 2006; 113(11):1625–1644. Review. [PubMed: 17039298]
44. Sarter M, Bruno JP. Developmental origins of the age-related decline in cortical cholinergic function and associated cognitive abilities. Neurobiol Aging. 2004; 25(9):1127–1139. Review. [PubMed: 15312959]
45. Bisiacchi PS, Borella E, Bergamaschi S, Carretti B, Mondini S. Interplay between memory and executive functions in normal and pathological aging. J Clin Exp Neuropsychol. 2008; 30(6):723–733. [PubMed: 18608665]
46. Busatto GF, Diniz BS, Zanetti MV. Voxel-based morphometry in Alzheimer's disease. Expert Rev Neurother. 2008; 8(11):1691–1702. Review. [PubMed: 18986240]
47. Ries ML, Carlsson CM, Rowley HA, Sager MA, Gleason CE, Asthana S, et al. Magnetic resonance imaging characterization of brain structure and function in mild cognitive impairment: a review. J Am Geriatr Soc. 2008; 56(5):920–934. [PubMed: 18410325]
48. Mufson EJ, Counts SE, Fahnestock M, Ginsberg SD. Cholinotrophic molecular substrates of mild cognitive impairment in the elderly. Curr Alzheimer Res. 2007; 4(4):340–350. Review. [PubMed: 17908035]
49. Sarter M, Bruno JP. Mild cognitive impairment and the cholinergic hypothesis: a very different take on recent data. Ann Neurol. 2002; 52(3):384–385. [PubMed: 12205659]
50. Herholz K, Weisenbach S, Kalbe E. Deficits of the cholinergic system in early AD. Neuropsychologia. 2008; 46(6):1642–1647. Review. [PubMed: 18201734]
51. Haense C, Kalbe E, Herholz K, Hohmann C, Neumaier B, Krais R, Heiss WD. Cholinergic system function and cognition in mild cognitive impairment. Neurobiol Aging. (in press) [Epub ahead of print].
52. Mazère J, Prunier C, Barret O, Guyot M, Hommet C, Guilloteau D, et al. In vivo SPECT imaging of vesicular acetylcholine transporter using [(123)I]-IBVM in early Alzheimer's disease. Neuroimage. 2008; 40(1):280–288. [PubMed: 18191587]
53. Barnes J, Whitwell JL, Frost C, Josephs KA, Rossor M, Fox NC. Measurements of the amygdala and hippocampus in pathologically confirmed Alzheimer disease and frontotemporal lobar degeneration. Arch Neurol. 2006; 63(10):1434–1439. [PubMed: 17030660]
54. Colliot O, Chételat G, Chupin M, Desgranges B, Magnin B, Benali H, et al. Discrimination between Alzheimer disease, mild cognitive impairment, and normal aging by using automated segmentation of the hippocampus. Radiology. 2008; 248(1):194–201. [PubMed: 18458242]
55. Du AT, Schuff N, Amend D, Laakso MP, Hsu YY, Jagust WJ, et al. Magnetic resonance imaging of the entorhinal cortex and hippocampus in mild cognitive impairment and Alzheimer's disease. J Neurol Neurosurg Psychiatry. 2001; 71(4):441–447. [PubMed: 11561025]

56. Barnes J, Bartlett JW, van de Pol LA, Loy CT, Scahill RI, Frost C, et al. A meta-analysis of hippocampal atrophy rates in Alzheimer's disease. Neurobiol Aging. 2009; 30(11):1711–1723. Review. [PubMed: 18346820]

57. Nagahara AH, Bernot T, Moseanko R, Brignolo L, Blesch A, Conner JM. Long-term reversal of cholinergic neuronal decline in aged non-human primates by lentiviral NGF gene delivery. Exp Neurol. 2009; 215(1):153–159. [PubMed: 19013154]

58. Tuszynski MH, Thal L, Pay M, Salmon DP, U HS, Bakay R, et al. A phase 1 clinical trial of nerve growth factor gene therapy for Alzheimer disease. Nat Med. 2005; 11(5):551–555. [PubMed: 15852017]

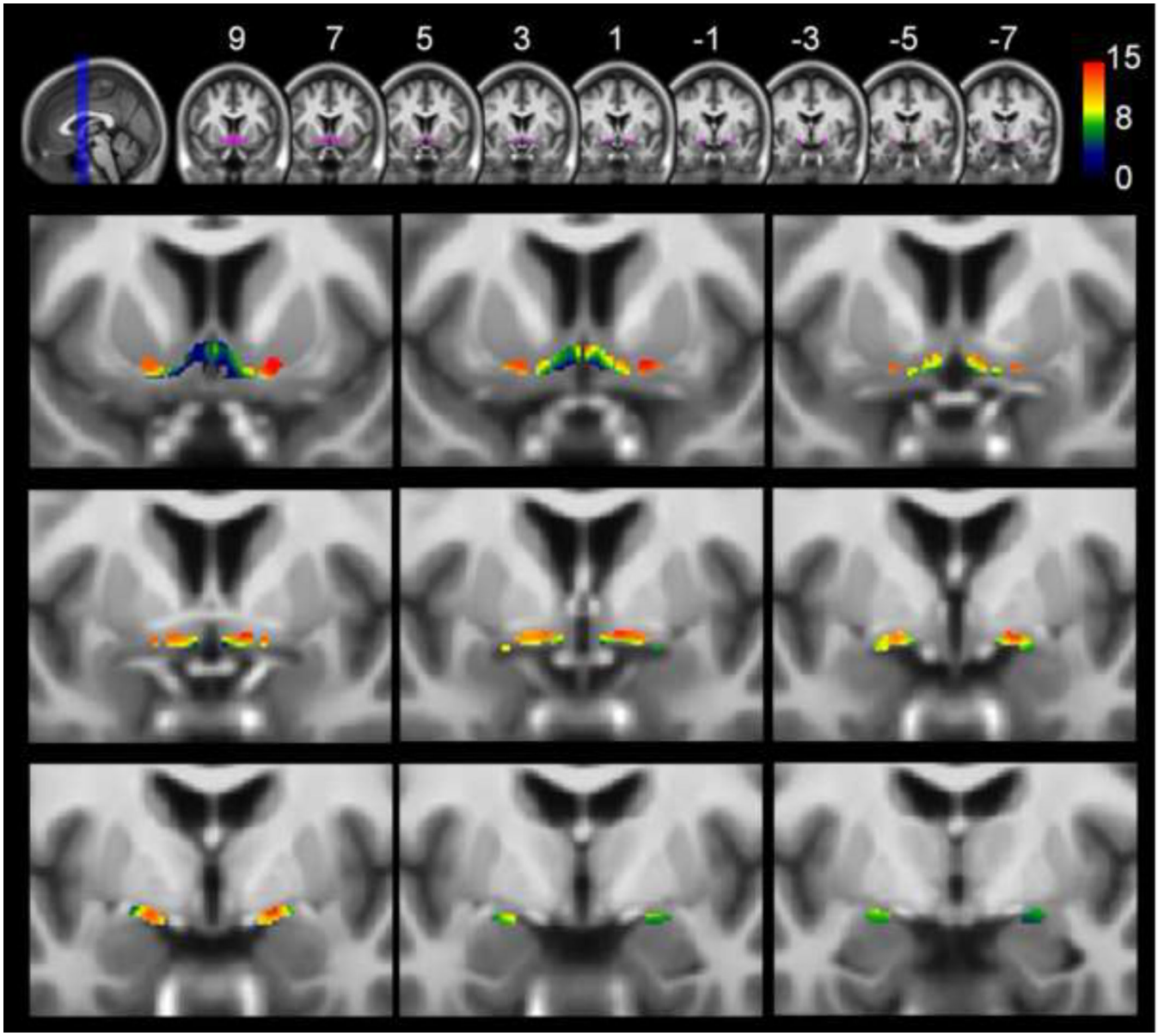

Figure 1. Age-related atrophy of the basal forebrain cholinergic system (BFCS)

Upper row: Overview of the basal forebrain cholinergic system region of interest (BFCS-ROI) (purple) projected onto coronal slices of the lifespan template in MNI space (MNI-coordinates y = 9 to y = −7 in intervals of 2mm). Lower rows: Results of the voxel-wise analysis restricted to the BFCS-ROI projected onto the same coronal slices and magnified to better represent the basal forebrain (running from y = 9 in upper left corner to y = −7 in lower right corner). Results of the voxel-wise analysis restricted to the BFCS-ROI are corrected for total intracranial volume and gender and are thresholded at $p<0.01$, FDR-corrected. A minimum cluster extension threshold of 5 contiguous voxels was applied. Statistical significance (in terms of T-values, 209 degrees of freedom) is coded by a color-scale from black-blue to red. Negative age-effects on grey matter volume are seen throughout the whole BFCS-ROI, being statistically most robust in anterior (lateral and medial) and intermediate parts of the nucleus basalis meynert (Ch4al, Ch4am, Ch4i).

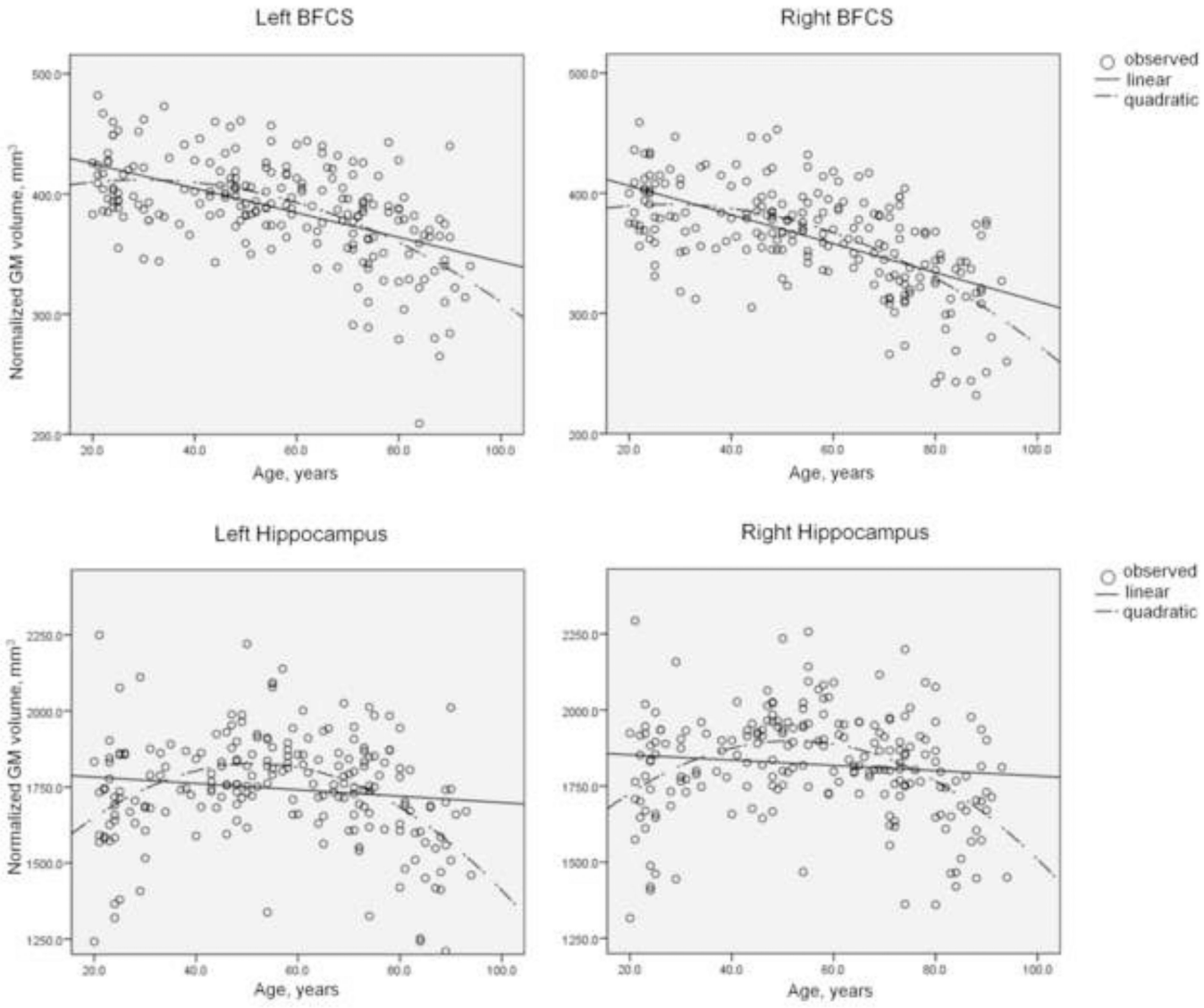

Figure 2. Plots of individual basal forebrain cholinergic system and hippocampus grey matter volumes against age

Individual left and right hemispheric hippocampus and basal forebrain cholinergic system (BFCS) grey matter (GM) volumes of the healthy cohort are plotted against age (circles). Linear and quadratic trends are shown by continuous and interrupted lines, respectively. The plots indicate stable (or even increasing) hippocampus GM volumes until middle-age and subsequent non-linear decline at advanced age. On the other hand, decline of BFCS GM volumes can be seen from early adulthood on and aggravates at advanced age.

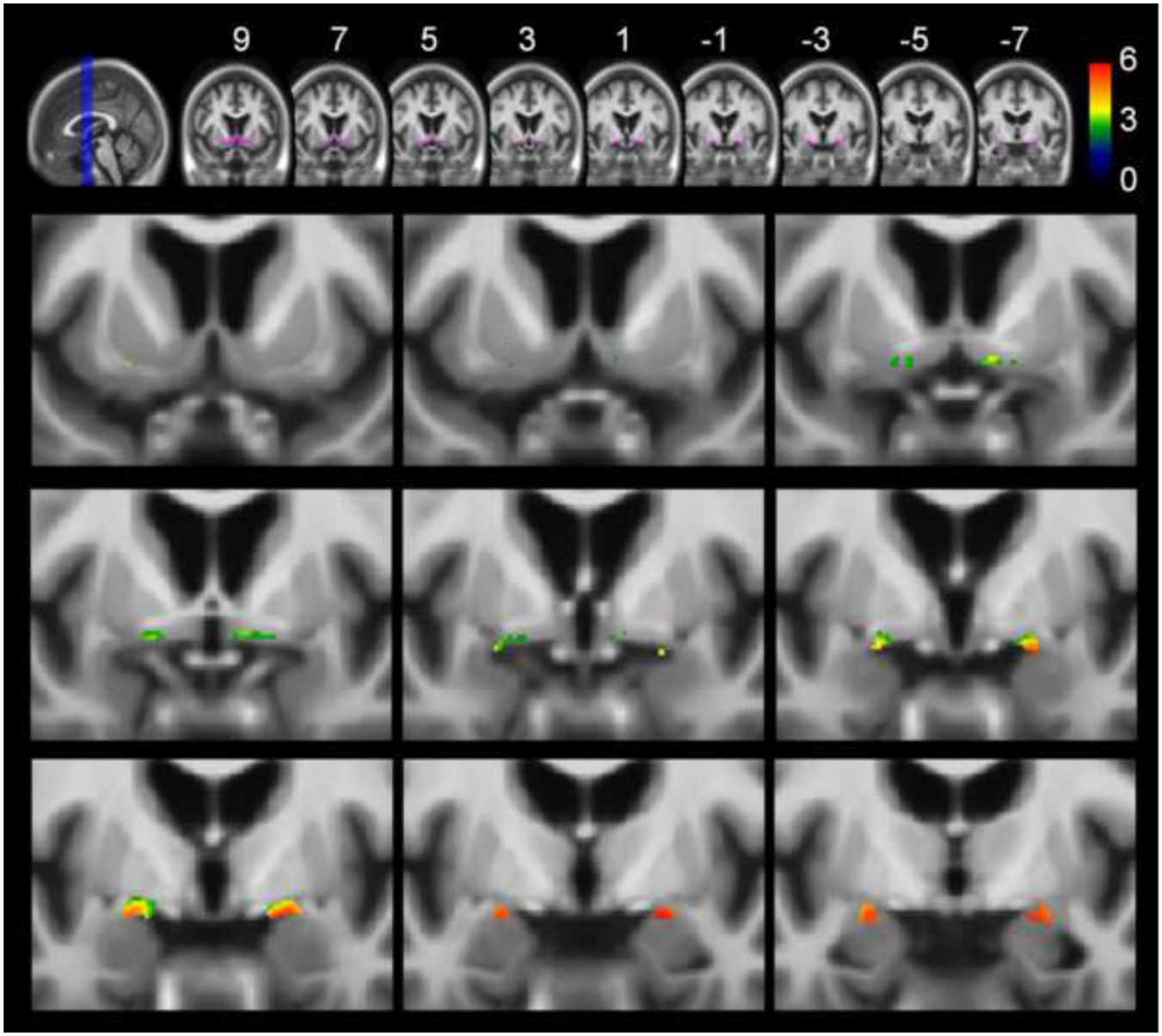

Figure 3. Atrophy of the basal forebrain cholinergic system (BFCS) in vmAD compared to healthy elderly controls

Upper row: Overview of the basal forebrain cholinergic system region of interest (BFCS-ROI) (purple) projected onto coronal slices of the elderly-AD template in MNI space (MNI-coordinates y = 9 to y = −7 in intervals of 2mm). Lower rows: Results of the voxel-wise analysis restricted to the BFCS-ROI projected onto the same coronal slices and magnified to better represent the basal forebrain (running from y = 9 in upper left corner to y = −7 in lower right corner). Results of the voxel-wise analysis restricted to the BFCS-ROI are corrected for total intracranial volume, age and gender and thresholded at $p<0.01$, FDR-corrected. A minimum cluster extension threshold of 5 contiguous voxels was applied. Statistical significance (in terms of T-values, 189 degrees of freedom) is coded by a color-scale from black-blue to red. Voxel-wise effects of reduced grey matter volume in vmAD compared to age-matched controls are restricted to the nucleus basalis Meynert (NBM).

Findings are statistically most robust in posterior parts of the NBM but extend also into intermediate and anterior medial regions.

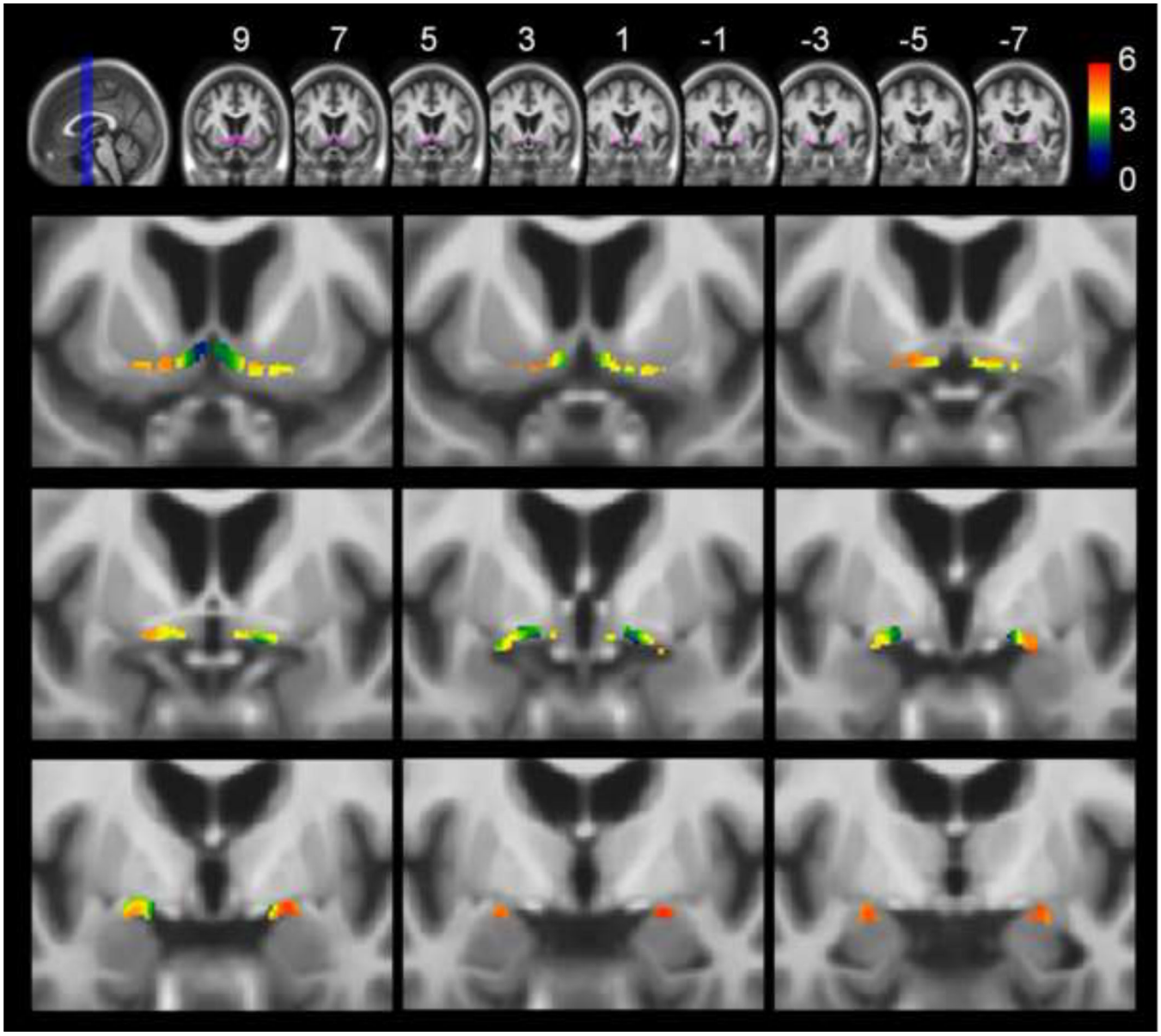

Figure 4. Atrophy of the basal forebrain cholinergic system in AD compared to healthy elderly controls

Upper row: Overview of the basal forebrain cholinergic system region of interest (BFCS-ROI) (purple) projected onto coronal slices of the elderly-AD template in MNI space (MNI-coordinates y = 9 to y = −7 in intervals of 2mm). Lower rows: Results of the voxel-wise analysis restricted to the BFCS-ROI projected onto the same coronal slices and magnified to better represent the basal forebrain (running from y = 9 in upper left corner to y = −7 in lower right corner). Results of the voxel-wise analysis restricted to the BFCS-ROI are corrected for total intracranial volume, age and gender and thresholded at $p<0.01$, FDR-corrected. A minimum cluster extension threshold of 5 contiguous voxels was applied. Statistical significance (in terms of T-values, 189 degrees of freedom) is coded by a color-scale from black-blue to red. Voxel-wise effects of reduced grey matter volumes in AD compared to age-matched controls are more widespread than in the vmAD group and are seen throughout the whole BFCS-ROI, including the rostral nuclei of the diagonal band of

Broca (Ch2, Ch3) and the whole extend of the nucleus basalis (NBM, Ch4). Similar to the vmAD group, effects are statistically most robust over posterior parts of the NBM.

Table 1

Group differences in hippocampus and BFCS grey matter volume as diagnostic markers

	HE	vmAD	AD	vmAD vs HE		AD vs HE	
				p	AUC	p	AUC
Hippocampus (bilat.)	3088±268	2770±354	2648±450	<.001	.78	<.001	.81
L Hippocampus	1494±142	1353±174	1288±207	<.001	-	<.001	-
R Hippocampus	1594±140	1.417±204	1359±256	<.001	-	<.001	-
BFCS (bilat.)	729±84	679±78	623±100	<.001	.69	<.001	.81
L BFCS	380±44	356±44	327±54	<.001	-	<.001	-
R BFCS	349±43	324±40	296±53	<.001	-	<.001	-
Comp (bilat.)	851±75	777±81	728±103	<.001	.76	<.001	.87
L Comp	435±40	400±43	374±51	<.001	-	<.001	-
R Comp	416±38	377±44	354±58	<.001	-	<.001	-

Values for hippocampus and BFCS (basal forebrain cholinergic system) are mean TIV-normalised grey matter volumes in mm^3 ± standard deviation. Values for Comp (composite marker) are calculated as the arithmetic mean of the TIV-normalised BFCS and hippocampus GM volumes divided by their respective mask size. P-values indicate the statistical significance of differing group mean values as assessed by group-wise 2-sample t-tests. AD = group of clinically manifest Alzheimer´s disease. R/L = right/left. AUC = Area under the curve (of a ROC-analysis). TIV = total intracranial volume. vmAD = group with questionable/very mild Alzheimer´s disease. HE = healthy elderly.